



Preparation, *In-Vitro* Bioactivity And Mechanical Properties of Reinforced 45S5 Bioglass Composite With HA-ZrO₂ Powders

SUNIL PRASAD^{1*}, VIKAS KUMAR VYAS¹, KUMARI DEEPA MANI²,
MD. ERSHAD¹ and RAM PYARE¹

¹Department of Ceramic Engineering, Indian Institute of Technology (BHU), Varanasi-221005, India.

²Department of Zoology, Banaras Hindu University, Varanasi-221005, India.

*Corresponding author E-mail: sunilmnnt25@gmail.com

<http://dx.doi.org/10.13005/ojc/330328>

(Received: April 07, 2017; Accepted: May 05, 2017)

ABSTRACT

Bioglass(45S5)-Hydroxyapatite(HA)-Zirconia(ZrO₂) biocomposites were prepared and heat treated at 1000,1100,1200°C for 5 hour. Simulated body fluid (SBF) is used to immersed these samples for 1,3,7,14,21 days. Samples were characterized before and after immersion in simulated body fluid by using FTIR, X-ray diffraction (XRD) and scanning electron microscope (SEM). FTIR were used to observed the formation of hydroxyapatite layer (HA) on the surface of these bio composite samples. The pH of the SBF were measured by using pH meter at 1,3,7,14,21 days. Different techniques were used to measured various mechanical properties and it was found to increase with increasing HA(10,20,30,40 wt%) and ZrO₂ (5,10,15,20 wt%) content.

Keywords:Bioglass(45S5), Hydroxyapatite(HA),Zirconia, Biocomposites, Simulated body fluid (SBF), FTIR spectrometry.

INTRODUCTION

Hench glass 45S5¹ has been extensively used to repair hard and soft tissue bone because of their excellent bioactive properties. However, an incomplete conversion into a bone-like material undergo by these bio active materials which severely limits their use in biomedical application².45S5 Bioglass is generally used in making various biomedical devices, such as middle ear, dental implants etc. Due to the brittleness nature of

45S5 bio glass and relatively its low strength, the application in non-load bearing situations is limited³. This silicate-based bio active glass has very low degradation and It has been found that remains in our body approximately more than one year after implantation⁴. This bioglass(45S5) does not alone provide sufficient bio activity and mechanical strength due to this reason we need to reinforced this bio active glass with increasing content of HA and ZrO₂.

Chemical composition of HA has similar to inorganic mineral of our bone and teeth⁵⁻⁶. It has excellent biocompatibility and bio activity. HA offers excellent biocompatibility, bioactivity⁷, low density, low compressive strength and low hardness. It has also relatively low mechanical properties. Therefore the use of HA as a load bearing implant teeth is very limited. Due to these limitation there is a need to strengthening of HA without loosing its biocompatibility⁸. It was found that zirconia (ZrO_2) possess high mechanical strength and very low toxicity⁹⁻¹⁰. For this reason (ZrO_2) is widely used as a biomaterial for hipprosthesis¹¹⁻¹², tooth crowns¹³ and dental implants¹⁴ and it was formed as a new bone restoring material in future. Sintered zirconia (ZrO_2) has very high mechanical strength than a cortical bone therefore new class zirconia is used as a new bone restoring material¹⁵⁻¹⁶. Because of difference in strength, the amount of stress and frequent bone fracture may occur resulting in bonding to a host bone. Due to the poor affinity to cells and tissues of zirconia (ZrO_2), there is a need to make composite by HA and ZrO_2 mixed together in order to combine the biocompatibility of HA, high toughness and strength of ZrO_2 . It has been observed zirconia retain high mechanical strength and toughness with HA without affecting the biocompatibility of HA¹⁷⁻²¹. The changes in physicochemical properties of the material is due to decomposition of HA. Performance of implant material is affected by change in its density, solubility, resorption and biocompatibility during implantation in a living body. Therefore HA decay is an important problem, both from scientific and application point of view. It has been found that calcium present in hydroxyapatite can react with ZrO_2 transformed zirconia into cubic form which make it tough by this transformation²².

Further it was observed that HA- ZrO_2 composites have very improved strength and toughness as compared to monolithic HA itself²³⁻²⁶. It is well known that P_2O_5 act as a strong glass network former. Covalent bond is formed between PO_4 tetrahedra structures in chains or rings by bridging oxygens²⁷. It is also known that Na_2O and CaO were act as glass network modifiers and formed non-bridging oxygens (NBO) into the glass network²⁸. In environment Zr present as a common trace element or metallic Zr(IV) normally present in human bone and tissue as low in the

range of 2–10 mg/kg body weight with an estimated average daily intake in humans of ~2.6 mg. The toxicity of Zr has been assessed low to moderate in animals²⁹. Ceramics can be divided into two main groups that has been used as an implant material i.e. bioinert and bioactive. Bioinert ceramics, such as zirconia (ZrO_2) show no interaction with the surrounding and living tissue. However, bioactive ceramics such as calcium phosphates are forming bonds with living hard and soft tissue. Since it has the main inorganic constituent of bones and teeth. HA is the most interesting bioactive ceramics³⁰.

Partially stabilized zirconia (PSZ) is bioinert and has highest strength and fracture strength was mixed with HA to obtained a bioactive implants with increased mechanical properties³¹⁻³². Similarly other oxides, such as alumina(Al_2O_3)³³, titania(TiO_2)³⁴, and yttria(Y_2O_3)³⁵ were studied to prepare HA composites in different structures via several methods.

In present investigation to obtained high load bearing implants of BG-HA- ZrO_2 composites were prepared with increasing HA and ZrO_2 in base bioactive glass to make biocomposite. Structural *in-vitro* and mechanical properties of

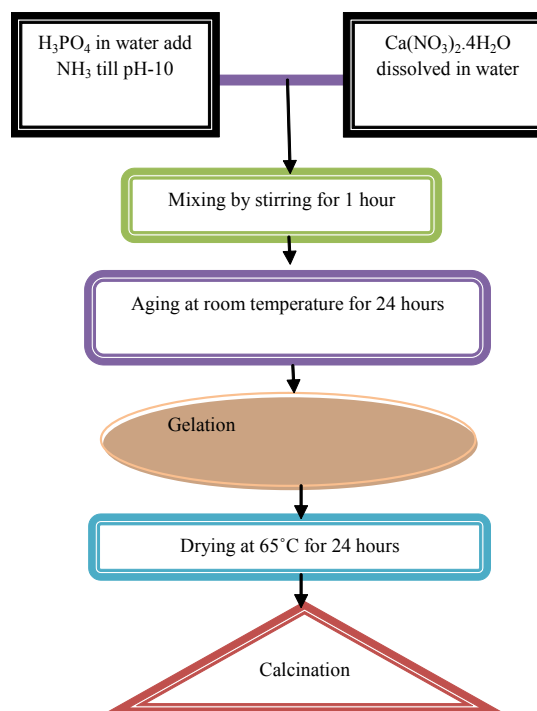


Fig.1: Flow chart of hydroxyapatite preparation by the sol-gel route

these biocomposite material were studied at different sintering temperature.

MATERIALS AND METHODS

Synthesis of BG-HA-ZrO₂ composites

45S5 Bioglass was prepared by using analytical grade quartz, calcium carbonate, sodium carbonate and ammonium dihydrogen orthophosphate by melting at 1400-1410°C with air as atmosphere and annealed in air oven at 500-550°C. Hydroxyapatite was prepared by solgel technique Fig.1. Bioglass (45S5), HA and ZrO₂ powder were milled and mixed by ball milling about 4 hours. Samples were placed and sintered in furnace at 1000, 1100 and 1200°C for 5 hours, rate of heating and cooling is at 5°C/minute. Uniaxial pressure of 100 MPa was applied to form rectangular bar shape sample of 4 mm×6 mm×40 mm size by using die of size 55 mm×10 mm. The composition of bioglass and biocomposites were illustrated in Table 1.

XRD Characterization

Cu-K α radiation at 40 kV/40mA was used to evaluate the presence of different phases through X-ray diffraction (XRD, Bruker D8) analysis. The scanning range of 2 θ angle was from 20° to 70° at scanning rate of 0.03809°/s with step size of 0.02°. The diffractograms were compared with JCPDS cards.

In-vitro analysis of biocomposites samples

At 37°C, the in vitro bioactivity evaluation of the biocomposite were determined by sample immersion in simulated body fluid (SBF) solutions for 1 to 21 days. SBF were prepared to determine *in-vitro* analysis of biocomposite samples. The SBF solution was prepared by Kokubo method³⁶ and compared ion

concentration (mM/litre) of SBF with human blood plasma solution which are shown in table 2. The composite samples in the form of circular pellet having the size of 1 cm diameter were immersed in SBF at 37°C. pH of the SBF solutions was measured by using digital pH meter (model-1611, ESICO-USA) for 1,3,7,14,21 days time periods.

Structural analysis of biocomposites by FTIR transmittance spectroscopy

Immersion of biocomposites in SBF before and after, formation of hydroxy carbonated apatite layer was formed on the surface and determined by FTIR (Shimadzu-8400S, Japan) used to record at the room temperature in the spectral range 4000-400 cm⁻¹.

Morphological analysis using scanning electron microscope (SEM) and EDS

The surfaces of bioactive composite were analyzed before and after immersion in SBF. These biocomposite samples were coated with gold plate before scanning of the sample with SEM. A scanning electron microscope (SEM-EV018, Carl Zeiss, UK) was used to analysis the surface microstructure of these samples before and after immersion in SBF. Elemental analysis were carried out by using energy dispersion spectrometry (EDS-51N1000, Oxford, UK)³⁷⁻⁴¹.

Physical and mechanical properties

Archimedes Principle was used to determine the density (Sartorius, Model: BP221S, USA) of these samples. UTM Machine (Tinius Olsen, H10KL, India) have been used to determine Compressive and toughness strength. Vickers micro hardness test was calculated using a micro hardness tester (HMV-2, Shimadzu, Japan) with a diamond

Table 1: Composition of Bioactive Glass and Biocomposites (BHZ1, BHZ2, BHZ3, BHZ4)

BG (45S5) Biocomposite Samples	Composition (wt %)			
	45SiO ₂ BG (45S5)	24.5Na ₂ O	24.5 CaO HA	6 P ₂ O ₅ ZrO ₂
BHZ1	85	10		5
BHZ2	70	20		10
BHZ3	55	30		15
BHZ4	40	40		20

indenter at 1.968N load for 30s. The average micro hardness was calculated by using formula. $HV=0.001854P/d^2$

RESULT

XRD analysis of bioactive composite sample.

The XRD pattern of sample BHZ1, BHZ2, BHZ3 and BHZ4 were presented in Fig.2, heated at 1000°C contained hydroxyapatite and tetragonal-zirconia phases. Upon heat treatment at higher temperatures i.e. 1100°C and 1200°C, the zirconia and wollastonite gradually transformed into zirconium silicate (zircon) respectively. Before and after soaking in SBF for various time periods i.e. 1, 3, 7, 14 and 21 days, typical XRD patterns were obtained on the surfaces of biocomposites. XRD patterns of the

biocomposite sample with HA(10,20,30,40wt%) and ZrO₂(5,10,15,20 wt%) is shown in the Fig.2(a-d). After immersion in SBF, crystalline peaks appear in the XRD patterns which indicates the formation of a crystalline layer on the surface of the bio composites. Initially well-defined hydroxyapatite (HA) peaks develop at (2θ) values of 23-27° of these composites after 3 days of soaking in SBF and ZrO₂ peaks develop at (2θ) values of 30-35° after 7 days of immersion.

The reaction between the HA and the ZrO₂ forms TCP and cubic ZrO₂ as follows⁴²:

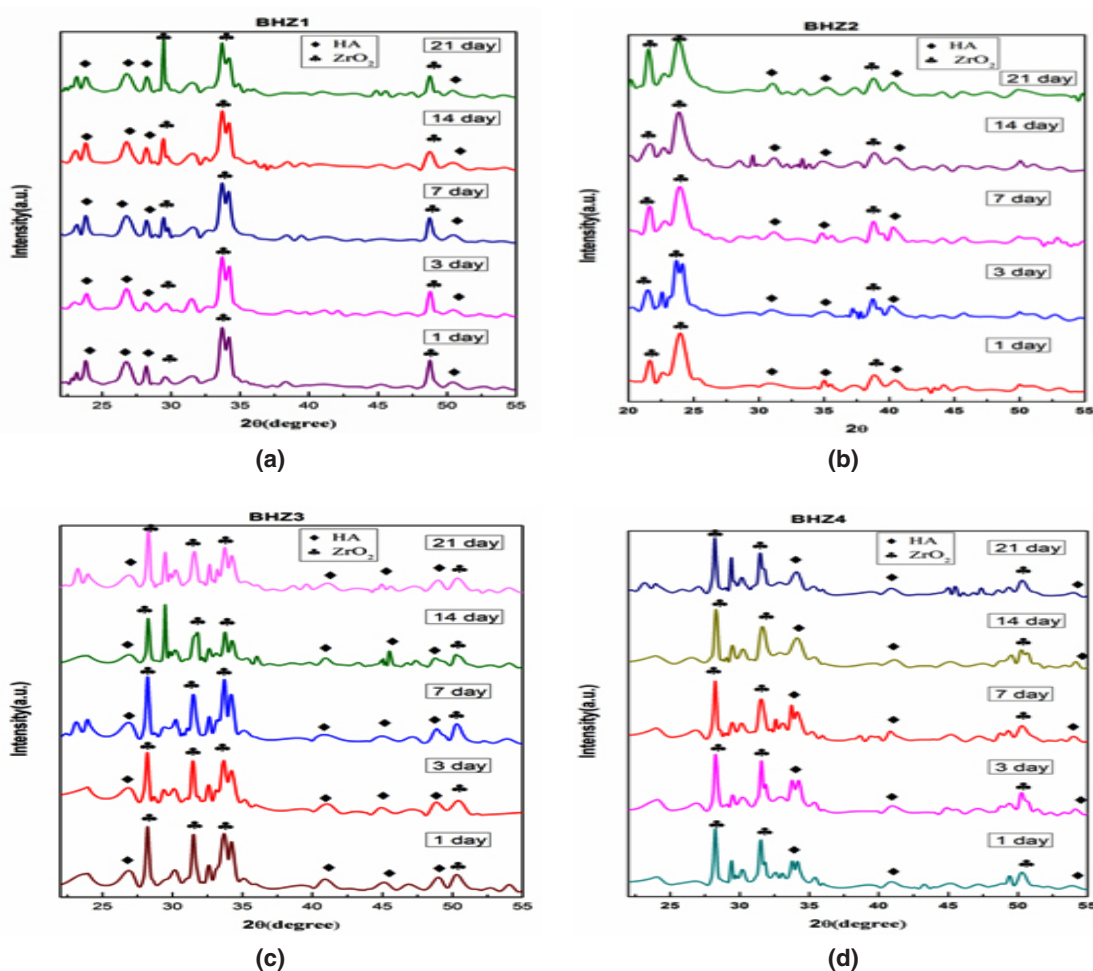
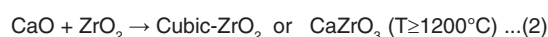
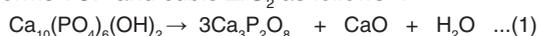


Fig. 2: (a,b,c,d) XRD pattern of biocomposite sample BHZ1, BHZ2, BHZ3 and BHZ4 after SBF treatment (1,3,7,14,21) days

Table 2: The ions concentration of SBF solution and human blood plasma (mM/litre)

S.No.	Ion	Simulated body fluid solution	Human blood plasma
1	Na ⁺	142.1	142.1
2	K ⁺	5.2	5.2
3	Mg ²⁺	1.6	1.6
4	Ca ²⁺	2.6	2.6
5	Cl ⁻	147.9	103.1
6	HCO ₃ ⁻	4.2	27.0
7	HPO ₄ ²⁻	1.1	1.1
8	SO ₄ ²⁻	0.6	0.6

Hydroxyapatite transforms into TCP by releasing calcium (or CaO) and water vapour as shown in equation (1). HA phase is not stable, and TCP is the major phase. According to reaction (2), the reaction continues, a lot of CaO is released, thus cubic-ZrO₂ are formed.

Transmission FTIR analysis of biocomposite sample

FTIR spectra bands of BHZ1 sample illustrated in Fig.3(a) for 3, 7, 14 and 21 days treated with SBF. At 516 and 639 cm⁻¹ P–O bending (crystalline) and P–O bending (amorphous) were formed. At 916 cm⁻¹ C–O stretching band shown which indicates the formation of HCA layer. The bands at about 1512 and 1695 cm⁻¹ were related to

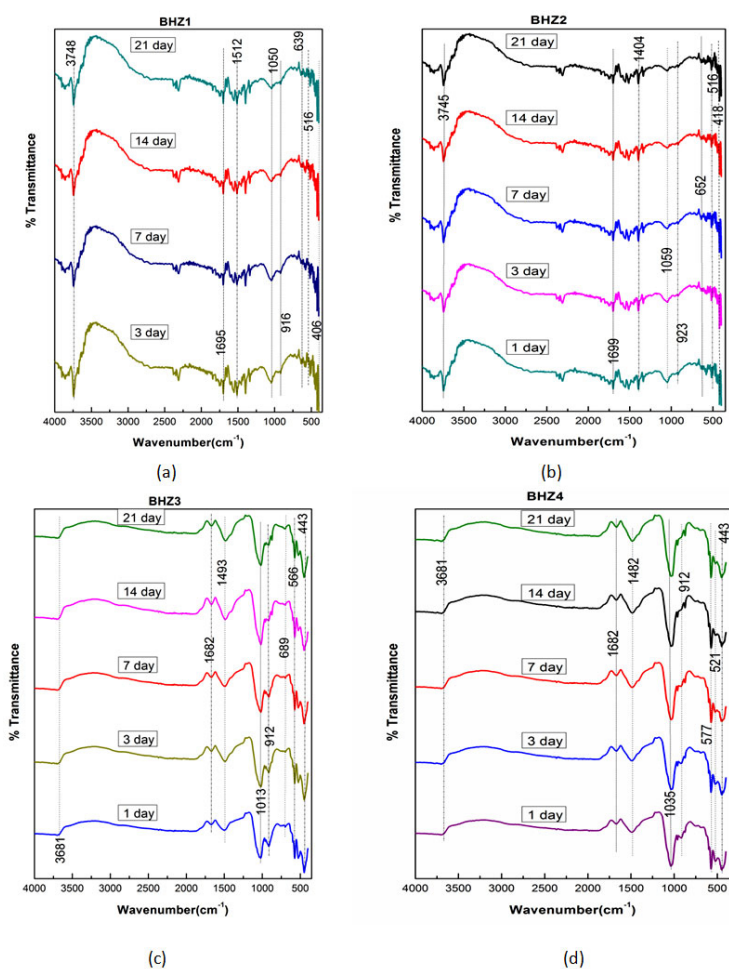


Fig.3: (a,b,c,d) FTIR of the biocomposite sample BHZ1, BHZ2, BHZ3 and BHZ4 after immersion in SBF treatment for (1,3,7,14,21) days

C–O (Stretch) and C=O (Stretch) modes respectively, and the broad band at about 3748 cm^{-1} are formed due to O–H groups on the surface. The samples in SBF for prolonged period indicates the similar response with small decrease in the intensities of the bands due to the formation of HCA layer. Further almost similar vibrations in all specimens (BHZ2, BHZ3, BHZ4) in Fig.3(b),(c),(d) which confirm apatite formation, these bands are also shown in table 3.

The samples in SBF for prolonged period shows the same response with small decrease in the intensities of the bands that resulted in the formation of HCA layer.

Zr can be react in two ways.

1. Zr as glass network modifier: Possibility of some splitting in Si-O-Si bonds leads to lower connectivity of the silicate network with increase in O/Si ratio in BHZ with respect to 45S5. This phenomenon results in decrease of bridging oxygens and with an increase in

non-bridging oxygens. However, after the incorporation of Zr, we found a significant reduction in the number of non-bridging oxygen in the FTIR spectra of the dried gels.

2. Zr as glass former: Zr may even act as a glass former with $[\text{ZrO}_4]^{4-}$ units occupying some positions of $[\text{SiO}_4]^{4-}$ tetrahedra. The extent of shifting the 29Si, resonance for a given tetrahedron is positive due to each covalent Si–O–Zr bridge⁴³.

pH analysis of biocomposite samples

Change in pH of biocomposite (BHZ1, BHZ2, BHZ3 and BHZ4) were presented in Fig.4 after immersing all samples in SBF for different time period. It was found that pH has increased upto 7 days due to the fast release of alkali ions (Na^+) and alkaline earth ions (Ca^{2+}) and its exchange with H^+ or H_3O^+ ions in the simulated body fluid (SBF) solution. There is increase in OH^- ions which increase the pH of the solution and breaking of Si-O-Si bonds which hold the glass structure together. Thus there is formation

Table 3: FTIR spectra bands of BHZ1, BHZ2, BHZ3, BHZ4 sample

Sample	P–O (crystalline)	P–O (amorphous)	C–O (Stretch)	C=O (Stretch)	O–H groups
BHZ1	516	639	916, 1512	1695	3748
BHZ2	516	652	923, 1404	1699	3745
BHZ3	566	689	912, 1493	1682	3681
BHZ4	521	577	912, 1482	1682	3681

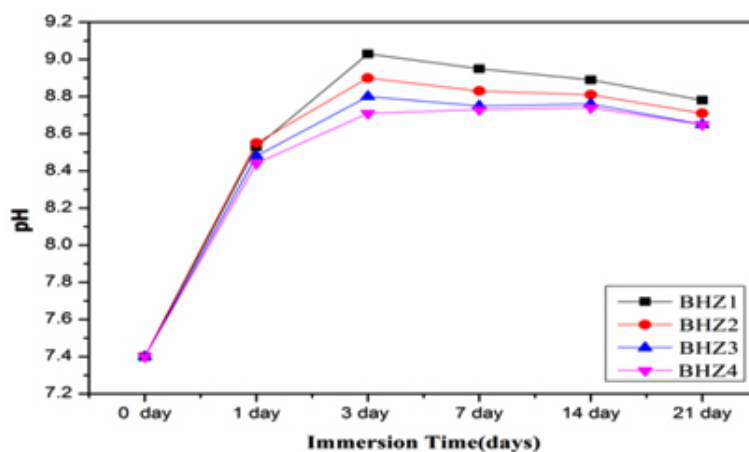
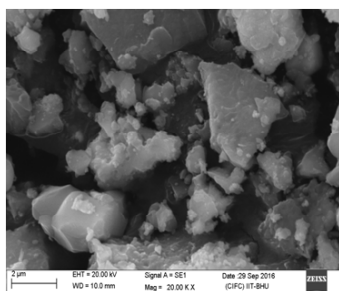


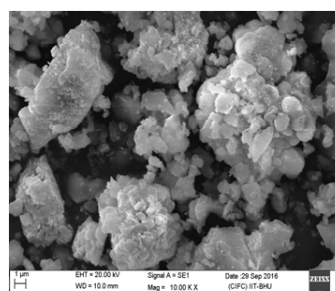
Fig. 4: pH behaviour of the SBF after immersion of the biocomposite samples (BHZ1, BHZ2, BHZ3, BHZ4)

of silanols which decrease the pH of the solution after 7 to 21 days. Soaking in SBF leads to the formation of an apatite layer on the surface of the composite samples depends upon the morphological properties of biocomposite sample⁴⁵⁻⁴⁶. *In vitro* hydroxyapatite

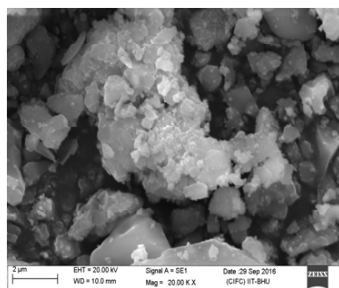
formation on body fluid inside simulated body fluid (SBF)⁴⁷ has four proposed stages. First: Fast cation exchange of Na^+ and Ca^{2+} with H^+ in solution, forming silanol bonds (Si-OH) on the glass surface i.e. $\text{Si-O-Na}^+ + \text{H}^+ + \text{OH}^- \rightarrow \text{Si-OH} + \text{Na}^+(\text{aq}) + \text{OH}^-$,



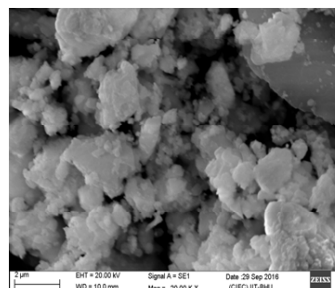
(a)



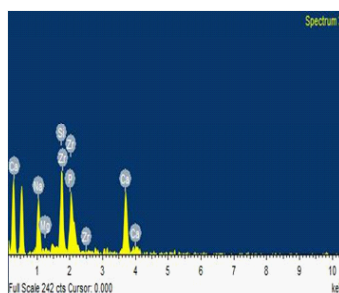
(b)



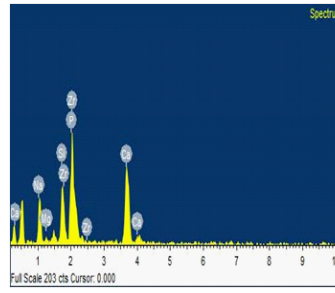
(c)



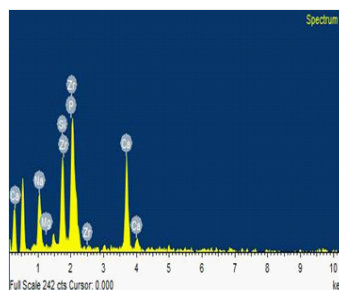
(d)



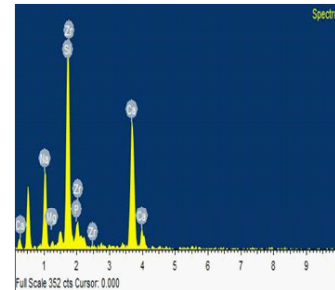
(e)



(f)



(g)



(h)

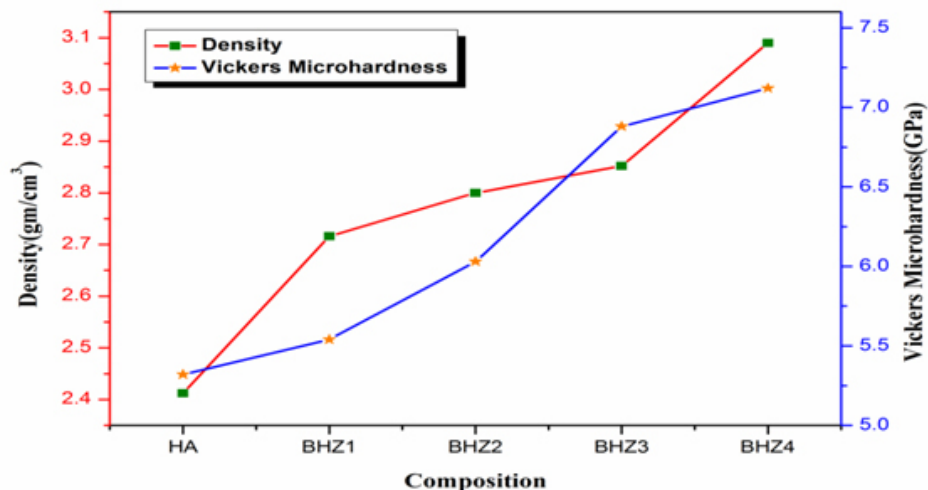
Fig.5: SEM of biocomposite samples after SBF (a-d) and EDX of biocomposite samples (e-h)

Second: A silica-rich (cation vacant) regions forms near the glass surface results increase in pH. Phosphate is also dissipated from the glass if available in the composition. Third: High local pH splits the Si-O-Si bonds and release OH⁻ which causes an attack to the silica glass network. Soluble silica dissolves in the solution in the form of Si(OH)⁴ and leaving more Si-OH (silanols) at the

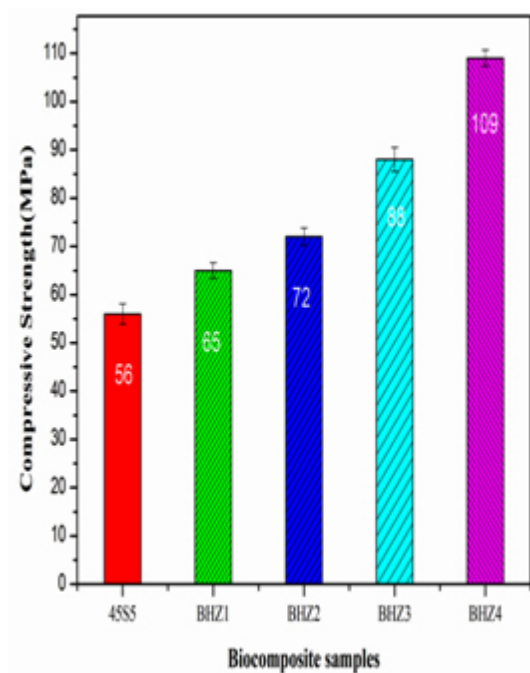
glass-solution interface: $\text{Si-O-Si} + \text{H}_2\text{O} \rightarrow \text{Si-OH} + \text{OH-Si}$, Fourth: Condensation of Si-OH groups near the glass surface due to re polymerization of the silica-rich layer.

SEM and EDS analysis of biocomposite sample after soaking in SBF

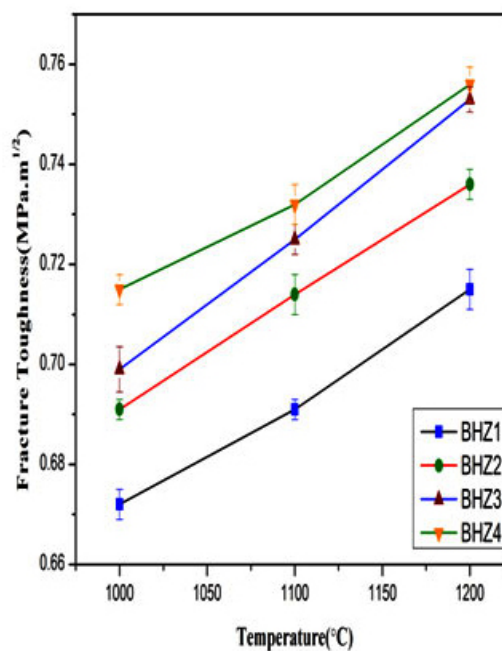
After *in vitro* studies the surface morphology



(a)



(b)



(c)

Fig.6: (a) Density and Vickers microhardness (b) Compressive strength (c) Fracture toughness of biocomposites (BHZ1, BHZ2, BHZ3 and BHZ4) sample

and hydroxyapatite layer formation on the surface of BHZ samples are shown using (SEM–EV018, Carl Zeiss, UK) Fig. 5(a-d). Before *in vitro* studies, a compact and uniform morphology is viewed for BHZ sample. Where BHZ samples obtained after 21 days of immersion in SBF, clear spherical apatite crystals were seen on the surface, which matches with the measured results⁴⁸. After *in vitro* studies, due to introduction of hydroxyapatite and ZrO₂ in BHZ sample a strong formation of HA layer on the sample surface took place. The above results shows that reactivity of BHZ sample is high in SBF samples. Fig. 5(e-h) shows the cross-sectional view and corresponding energy dispersive (EDS) spectra of BHZ sample after *in vitro* studies by using instrument (EDS–51N1000, Oxford, UK). The observed results show an embedded spherical hydroxyapatite layer on the surface of the biocomposite. Calcium and phosphate on the biocomposite surface is confirmed by EDS spectra of BHZ sample, which shows the presence of strong *in vitro* bioactivity.

Mechanical properties of BHZ biocomposites

Fig. 6(a) shows the density and micro hardness of biocomposite, this result shows increase in hydroxyapatite and zirconia content which leads to increase in density and hardness value. Fig. 6(b) and (c) shows the strength and fracture toughness of 45S5, BHZ1, BHZ2, BHZ3 and BHZ4 samples as a function of sintering temperature and found to increase with increasing sintering temperature. In Fig. 6(b) the strength of the 45S5, BHZ1, BHZ2, BHZ3 and BHZ4 composite samples was about 56MPa, 65MPa, 72MPa, 88MPa, 109MPa respectively. Sintering at 1000°C lowering the strength of the bodies due to insufficient compactness. With increasing sintering temperature to 1200°C the strength value increases due to complete compactness. The

fracture toughness show significant changes with the changing sintering temperature. The fracture toughness of the samples sintered at 1000°C, 1100°C and 1200°C were BHZ1(0.672, 0.691, 0.715 MPa.m^{1/2}), BHZ2(0.691, 0.714, 0.736 MPa.m^{1/2}), BHZ3(0.699, 0.725, 0.753 MPa.m^{1/2}) and BHZ4(0.715, 0.732, 0.756 MPa.m^{1/2}) respectively. Therefore, due to its superior strength and toughness, the samples sintered at 1200°C were chosen for a set of structural examinations.

CONCLUSION

The increasing amount of hydroxyapatite (10, 20, 30, 40wt%) and zirconia (5, 10, 15, 20 wt%) reinforced with base bio active glass upto the limit increase the bioactivity. Beyond 20wt%, addition of ZrO₂ causes a decrease in maxima of the pH of SBF solution containing immersed samples. Present investigation it was found that bio composite having 40wt% HA, 20wt% ZrO₂ and 40wt% bioactive glass have highest bioactivity, density, micro hardness, compressive strength and fracture toughness. Thus, we can say that reinforcement of HA+ZrO₂ in the 45S5 bioactive glass would be a good bioactive materials.

ACKNOWLEDGMENT

The authors gratefully thanks to Department of Ceramic Engineering, IIT (BHU) and Central Instrument Facility, IIT (BHU) Varanasi, India for providing required facilities for the present research work. The present work was supported by Rajiv Gandhi National Fellowship, University Grant Commission, New Delhi, India

REFERENCE

- Hench, L.L.; Splinter, R.J.; Allen, W.C.; Greenlee, T.K.; *J. Biomed. Mater. Res.* **1971**, *2*, 117.
- Hench, L.L.; *Bioceramics: From concept to clinic. J. Am. Ceram Soc.* **1991**, *74*, 1487-1510.
- Cao, W.; Hench, L.L.; *Bioactive Materials. Ceramics International* **1996**, *22*, 493-507.
- Hamadouche, M.; Meunier, A.; Greenspan, D.C.; Blanchat, C.; Zhong, J.P.; Torre, G.P. La; Sedel, L. J. *Biomed. Mater. Res.* **2001**, *54*, 560.
- Jarcho, M.; Kay, J.F.; Gumaer, K.I.; Doremus, R.H.; Drobeck, H.P.; *Tissue, cellular and subcellular events at a bone-ceramic hydroxylapatite interface. J. Bioeng.* **1977**, *1*(2), 79–92.
- Nayak, A.K.; *Hydroxyapatite synthesis methodologies: An overview. Int. J. Chem. Tech. Res.* **2010**, *2*(2), 903-7.

7. Hench, L.L.; Wilson, J. An Introduction to Bioceramics. World Scientific **1993**, 386.
8. Balani, K; Lahiri, D; Keshri, AK; Bakshi, SR; Tercero, JE; Agarwal, A; The nano-scratch behavior of biocompatible hydroxyapatite reinforced with aluminum oxide and carbon nanotubes. *Jom* **2009**, *61*(9), 63–6.
9. Sollazzo, V; Pezzetti, F; Scarano, A; Piattelli, A; Bignozzi, CA; Massari, L; Zirconium oxide coating improves implant osseo integration in vivo. *Dent Mater* **2008**, *24*, 357–61.
10. Albrektsson, T; Hansson, HA; Ivarsson, B; Interface analysis of titanium and zirconium bone implants. *Biomaterials* **1985**, *6*, 97–101.
11. Masonis, JL; Bourne, RB; Ries, MD; McCalden, RW; Salehi, A; Kelman, DC; Zirconia femoral head fractures: a clinical and retrieval analysis. *J. Arthroplast* **2004**, *19*, 898–905.
12. DeAza, AH; Chevalier, J; Fantozzi, G; Schehl, M; Torrecillas, R; Crack growth resistance of alumina, zirconia and zirconia toughened alumina ceramics for joint prostheses. *Biomaterials* **2001**, *23*, 937–45.
13. Kong, Y; Yang, Z; Zhang, G; Yuan, Q; Friction and wear characteristics of mullite, ZTM and TZP ceramics. *Wear* **1998**, *218*, 159–66.
14. Kohal, RJ; Wolkewitz, M; Mueller, C; Alumina-reinforced zirconia implants: survival rate and fracture strength in a masticatory simulation trial. *Clin. Oral Implants Res.* **2010**, *21*, 1345–52.
15. Atilgan, S; Erol, B; Yardimeden, A; Yaman, F; Ucan, MC; Gunes, N; A three dimensional analysis of reconstruction plates used in different mandibular defects. *Biotechnol/Biotechnol Equip.* **2010**, *24*, 1893–6.
16. Nisitani, H; Kim, YH; Goto, H; Nishitani, H; Effects of gage length and stress concentration on the compressive strength of a unidirectional CFRP. *EngFractMech* **1994**, *49*, 953–61.
17. Li, J; Liao, H; Hermansson, L; Sintering of partially-stabilized zirconia and partially-stabilized zirconia—hydroxyapatite composites by hot isostatic pressing and pressureless sintering. *Biomaterials* **1996**, *17*(18), 1787–90.
18. Silva, V V.; Lameiras, FS; Domingues, RZ; Microstructural and mechanical study of zirconia-hydroxyapatite (ZH) composite ceramics for biomedical applications. *Compos .Sci.Technol.* **2001**, *61*, 301–10.
19. Delgado, JA; Morejón, L; Martínez, S; Ginebra, MP; Carlsson, N; Fernández, E; Zirconia-toughened hydroxyapatite ceramic obtained by wet sintering. *J. Mater Sci. Mater Med.* **1999**, *10*(12), 715–9.
20. Kong, Y-M; Kim, S; Kim, H-E; Lee, I-S.; Reinforcement of Hydroxyapatite Bioceramic by Addition of ZrO₂ Coated with Al₂O₃. *J. Am. Ceram Soc.* **2004**, *82*(11), 2963–8.
21. Takagi, M; Mochida, M; Uchida, N; Saito, K; Uematsu, K.; Filter cake forming and hot isostatic pressing for TZP-dispersed hydroxyapatite composite. *J. Mater Sci. Mater Med.* **1992**, *3*(3), 199–203.
22. Li, J; Hermansson, L; Söremark, R; High-strength biofunctional zirconia: mechanical properties and static fatigue behaviour of zirconia-apatite composites. *J. Mater Sci. Mater Med.* **1993**, *4*(1), 50–54.
23. Zhang, J; Iwasa, M; Kotobuki, N; Tanaka, T; Hirose, M; Ohgushi, H; Fabrication of Hydroxyapatite Zirconia Composites for Orthopedic Applications. *J. Am. Ceram Soc.* **2006**, *89*(11), 3348–55.
24. Khalil, KA; Kim, SW; Kim, HY; Consolidation and mechanical properties of nanostructured hydroxyapatite (ZrO₂+3mol% Y₂O₃) bioceramics by high-frequency induction heat sintering. *Mater Sci. Eng. A.* **2007**, *456*(1-2), 368–72.
25. Rapacz-Kmita, A; Ióśczyk, A; Paszkiewicz, Z; Mechanical properties of HAp–ZrO₂ composites. *J Eur Ceram Soc.* **2006**, *26*(8), 1481–89.
26. Wu; Jenn-Ming; T-SY; Sintering of hydroxylapatite-zirconia composite materials. *J. Mater Sci.* **1988**, *23*(10), 3771–78.
27. Little flower, G; Reddy, M. Srinivasa; Reddy, M.V. Ramana; Veeraiyah, N.; *Naturforsch, Z.; A: Phys. Sci.* **2007**, *62*, 315.
28. Reddy, M. Srinivasa ; NagaRaju, G.; Nagarjuna, G.; Veeraiyah, N. ; *J. Alloys Comp.* **2007**, *41*, 438.
29. Ghosh, S. ; Sharma, A.; Talukder, G.; *Biol. Trace Elem. Res.* **1992**, *35*, 247.
30. Vallet-Regi, M; González-Calbet, J.M.; Calcium phosphates as substitution of bone

- tissues. *Prog. Solid State Chem.* **2004**, *32*, 1–31.
31. Shen, Z.J.; Adolfsson, E.; Nygren, M.; Gao, L.; Kawaoka, H.; Niihara, K.; Densehydroxyapatite–zirconia ceramic composites with high strength for biological applications. *Adv.Mater.* **2001**, *13*, 214–216.
32. Silva, V.V.; Domingues, R.Z.; Lameiras, F.S.; Microstructural and mechanical study of zirconia-hydroxyapatite(ZH) composite ceramics for biomedical applications. *Compos. Sci. Technol.* **2001**, *61*, 301–310.
33. Zhang, C.; Zhang, X.; Liu, C.; Sun, K.; Yuan, J.; Nano-alumina/hydroxyapatite composite powders prepared by in-situ chemical precipitation. *Ceram.Int.* **2016**, *42*, 279–285.
34. Milella, E.; Cosentino, F.; Licciulli, A.; Massaro, C.; Preparation and characterisation of titania/hydroxyapatite composite coatings obtained by sol–gel process. *Biomaterials* **2001**, *22*, 1425–1431.
35. Parente, P.; Sanchez-Herencia, A.J.; Mesa-Galan, M.J.; Ferrari, B.; Functionalizing Ti-Surfaces through the EPD of hydroxyapatite/nanoY2O3. *J.Phys.Chem.*, **2012**, B 117, 1600–1607.
36. Kokubo, T.; Kushitani, H.; Sakka, S.; Kitsugi, T.; Yamamuro, T.; Solutions able to reproduce in vivo surface-structure changes in bioactive glass-ceramics A-W. *Journal of Biomedical Materials Research* **1990**, *24*, 721-734.
37. Tampieri, A.; D'Alessandro, T.; Sandri, M.; Sprio, S.; Landi, E.; Bertinetti, L.; Panseri, S.; Peponi, G.; Goettlicher, J.; Bañobre-López, M.; Rivas, J.; Intrinsic magnetism and hyperthermia in bioactive Fe-doped hydroxyapatite. *Acta Biomater.* **2012**, *8* (2), 843–851.
38. Fujibayashi, S.; Neo, M.; Kim, H.M.; Kokubo, T.; Nakamura, T.; A comparative study between in vivo bone in growth and in vitro apatite formation on Na₂O–CaO–SiO₂ glasses. *Biomaterials* **2003**, *24*, 1349–1356.
39. Clupper, D.C.; Gough, J.E.; Embanga, P.M.; Notingher, I.; Hench, L.L.; Hall, M.; Bioactive evaluation of 45S5 bioactive glass fibres and preliminary study of human osteoblast attachment. *J. Mater. Sci. Mater. Med.* **2004**, *15*, 803–808.
40. Kokubo, T.; Surface chemistry of bioactive glass-ceramics. *J. Non-Cryst. Solids* **1990**, *120*, 138–151.
41. Kim, H.; Miyaji, F.; Kokubo, T.; Kokubo (1995). Bioactivity of Na₂O–CaO–SiO₂ glasses. *J. Am. Ceram. Soc.* **1995**, *79* (9), 2405–2411.
42. Wu, J.M.; Yeh, T.S.; Sintering of hydroxylapatite–zirconia composite materials. *J. Mater. Sci.* **1988**, *23*, 3771.
43. Barbieri, L.; Cannillo, V.; Leonelli, C.; Montorsi, M.; Mustarelli, P.; Siligardi, C.; Experimental and MD simulations study of CaO–ZrO₂–SiO₂ glasses. *J.Phys.Chem.B* **2003**, *107*, 6519–6525.
44. Greenspa, DC; L.L. Hench; Chemical and mechanical behavior of bioglass coated alumina. *J. Biomed Materials Res.* **1976**, *10*, 503-509.
45. Satoshi, H.; Kanji, T.; Chikara, O.; Akiyoshi, O.; Mechanism of Apatite Formation on a Sodium Silicate Glass in a Simulated Body Fluid. *J. Am Ceram Soc.* **1999**, *82*, 2155-2160.
46. Toshihiro, K.; Yoshimasa, H.; Masayuki, N.; Mitsuo, N.; Apatite Formation on Calcium Phosphate Invert Glasses in Simulated Body Fluid. *J. Am Ceram Soc.* **2001**, *84*, 450-452.
47. Clark, AE; Pantano, CG; Hench, L.L.; Auger spectroscopic analysis of Bioglass corrosion films. *J. Am Ceram Soc.* **1976**, *59*, 37-39.
48. P.Li, Ohtuki, C.; Kokubo, T.; Nakanishi, K.; Soga, N.; Nakamura, T.; Yamamuro, T.; Effects of ions in aqueous media on hydroxyapatite induction by silica gel and its relevance to bioactivity of bioactive glasses and glass-ceramics. *J. Appl. Biomater.* **1993**, *4*, 221–229.